Frontiers in Bioscience Landmark

Front. Biosci. (Landmark Ed) **2025**; 30(12): 46123
https://doi.org/10.31083/FBL46123

Original Research

Active Vitamin D Insufficiency Accelerates Skeletal Aging via Oxidative Stress and p16-Mediated Senescence

Wanxin Qiao[1], Mingxin Huang[1], Lulu Chen[1], David Goltzman[2], Dengshun Miao[1,3,*]

[1]The Research Center for Bone and Stem Cells, Department of Anatomy, Histology and Embryology, Nanjing Medical University, 211166 Nanjing, Jiangsu, China
[2]Calcium Research Laboratory, McGill University Health Centre and Department of Medicine, McGill University, Montreal, QC H4A 3J1, Canada
[3]Department of Plastic Surgery, Affiliated Friendship Plastic Surgery Hospital of Nanjing Medical University, 210029 Nanjing, Jiangsu, China
*Correspondence: dsmiao@njmu.edu.cn (Dengshun Miao)

Academic Editor: Ioanna-Katerina Aggeli
Submitted: 28 August 2025 Revised: 7 November 2025 Accepted: 21 November 2025 Published: 25 December 2025

Abstract

Background: Vitamin D is essential for skeletal health, but its role in redox homeostasis and cellular senescence during aging *in vivo* is unclear. We therefore investigated whether active vitamin D insufficiency accelerates bone loss via oxidative stress and senescence pathways. **Methods**: Male wild-type (WT) and Cyp27b1 haploinsufficient mice (modeling vitamin D insufficiency) were treated with N-acetylcysteine (NAC) or 1,25-dihydroxyvitamin D_3 [1,25$(OH)_2D_3$]. Double-mutant $p16^{-/-}Cyp27b1^{+/-}$ mice were used to assess the role of the tumor suppressor protein p16. Mice were maintained until 8 months of age in a specific pathogen-free facility. Outcomes included lifespan (n = variable per group, monitored daily); generation of oxidative stress (determined by serum malondialdehyde [MDA] levels via assay kit); generation of bone reactive oxygen species [ROS] (determined via flow cytometry), development of DNA damage (indicated by 8-hydroxy-2′-deoxyguanosine [8-OHdG] and γ-H2A.X generation and determined via immunohistochemistry and Western blot); and senescence (assessed by generation of β-galactosidase [β-gal], p16, and senescence-associated secretory phenotype [SASP] cytokines as determined via staining, blot, and real-time reverse transcription polymerase chain reaction). Additionally, bone microarchitecture was examined via micro-computed tomography and histomorphometry. Data from at least 5 mice per group were analyzed using unpaired Student's *t*-test for two-group comparisons and two-way analysis of variance for multi-group comparisons, with significance at $p < 0.05$. **Results**: Compared with wild-type controls, $Cyp27b1^{+/-}$ mice showed a significantly shorter lifespan, higher oxidative stress, greater DNA damage, increased senescence markers, and lower trabecular bone volume (all $p < 0.05$). In $Cyp27b1^{+/-}$ mice, treatment with either N-acetylcysteine or 1,25$(OH)_2D_3$ significantly improved survival, reduced oxidative stress and DNA damage, attenuated senescence markers, and increased bone volume relative to untreated $Cyp27b1^{+/-}$ mice ($p < 0.05$ for all relevant comparisons; n = 5 per group). Genetic deletion of p16 in $Cyp27b1^{+/-}$mice similarly increased bone volume and reduced senescence-associated readouts compared with $Cyp27b1^{+/-}$ controls ($p < 0.05$; n = 5). **Conclusions**: Active vitamin D insufficiency accelerates skeletal aging *in vivo* through a pathway involving reactive oxygen species-DNA damage-p16/senescence-associated secretory phenotype. Antioxidants, vitamin D repletion, or p16 inhibition rescued bone loss, highlighting redox-senescence axes as potential therapeutic targets for osteoporosis.

Keywords: vitamin D; oxidative stress; p16 tumor suppressor protein; cellular senescence; osteoporosis; N-acetylcysteine

1. Introduction

Osteoporosis and age-related skeletal fragility remain major public health challenges driven by an imbalance between bone formation and resorption that emerges with aging [1,2]. Accumulating evidence implicates oxidative stress and cellular senescence as central, convergent mechanisms that impair osteoblast function, enhance osteoclastogenesis, and damage bone microarchitecture [3–6]. In parallel, vitamin D signaling via the vitamin D receptor (VDR) contributes to skeletal health not only through mineral homeostasis but also by modulating redox balance, DNA damage responses, and inflammatory programs in bone cells [7–10]. However, how insufficiency of active vitamin D (1,25$(OH)_2D_3$) integrates with oxidative stress to trigger p53–p21 and $p16^{INK4a}$ checkpoints, establish a stable senescence-associated secretory phenotype (SASP), and accelerate skeletal aging *in vivo* remains incompletely defined.

In the aging skeleton, reactive oxygen species (ROS) activate the DNA damage response and checkpoint pathways that can culminate in senescence, with p21 often marking an initial arrest and $p16^{INK4a}$ enforcing a more durable state linked to SASP-mediated paracrine effects on bone remodeling [3–6,11,12]. Independent studies demonstrate that enhancing antioxidant defenses or targeting senescent cells improves bone mass and strength in preclinical models, underscoring the therapeutic potential of redox–senescence modulation [4,13,14]. Vitamin D/VDR signaling intersects with chromatin remodeling and cell-cycle regulators and has been reported to influence oxidative stress handling in multiple cell lineages, suggesting

a plausible route by which active vitamin D sufficiency might restrain senescence initiation and maintenance in bone [9,10,15–19]. Yet, direct *in vivo* evidence connecting active vitamin D insufficiency to increased skeletal ROS, DDR activation, and a transition from p21- to p16-dominant senescence programs is limited.

Here, using genetic and pharmacological perturbations, we delineate a vitamin D–redox–senescence axis that controls skeletal remodeling *in vivo*. We show that active vitamin D insufficiency elevates ROS, suppresses nuclear factor erythroid 2-related factor 2 (Nrf2)/superoxide dismutase 1 (SOD1) defenses, and increases DNA damage in bone, leading to augmented p16-associated senescence and SASP, impaired osteoblastogenesis, and increased osteoclast activity. Antioxidant supplementation or $1,25(OH)_2D_3$ repletion reverses these changes, and genetic reduction of p16 attenuates bone loss by rebalancing formation and resorption. These findings integrate and extend prior observations on redox and senescence in skeletal aging and position active vitamin D sufficiency as a modifiable upstream determinant of bone health in aging.

2. Materials and Methods

2.1 Animal Experiments

Cyp27b1$^{+/-}$ mice were generated by intercrossing heterozygous parents and genotyped using established protocols [20]. The *p16*$^{-/-}$ knockout mice were kindly provided by Baojie Li (Shanghai Jiao Tong University, Shanghai, China). The *Cyp27b1*$^{+/-}$*p16*$^{-/-}$ double mutant mice were produced by sequential breeding of *Cyp27b1*$^{+/-}$ and *p16*$^{-/-}$ mouse lines. After weaning at postnatal day 21, *Cyp27b1*$^{+/-}$ mice were randomly assigned to one of three intervention groups, with wild-type (WT) mice serving as controls. Group 1 received a standard rodent chow diet and sterile drinking water. To prevent oxidation, group 2 was administered the antioxidant N-acetylcysteine (NAC; 1 mg/mL) in drinking water, which was refreshed every 48 hours. Group 3 received subcutaneous injections of $1,25(OH)_2D_3$ (0.1 µg/kg body weight) every other day, prepared in ethanol and diluted in sterile phosphate-buffered saline (PBS; final ethanol concentration <5%). All mice were maintained in a specific pathogen-free (SPF) facility at the Animal Experiment Center of Nanjing Medical University, with a 12-hour light/dark cycle, controlled temperature (22–24 °C), and ad libitum access to food and water. Mice were monitored for body weight, behavior, and signs of distress weekly and survival time was recorded until all *Cyp27b1*$^{+/-}$ mice had succumbed. At 8 months of age, mice were anesthetized via intraperitoneal injection of a mixture of ketamine (80 mg/kg, 100 mg/mL) and xylazine (10 mg/kg, 20 mg/mL) mixture, and following deep anesthesia, were euthanized by cervical dislocation in accordance with AVMA guidelines. For lifespan analyses, we monitored n = 10 WT, 36 = XX *Cyp27b1*$^{+/-}$, n = 22 *Cyp27b1*$^{+/-}$+NAC, and n = 8 *Cyp27b1*$^{+/-}$+$1,25(OH)_2D_3$ mice until natural death. For cross-sectional analyses at 8 months of age (biochemistry, histology, micro-CT, Western blot, and RT–PCR), a separate cohort of n = 5 mice per group (WT, *Cyp27b1*$^{+/-}$, *Cyp27b1*$^{+/-}$+NAC, *Cyp27b1*$^{+/-}$+$1,25(OH)_2D_3$) was euthanized for tissue and serum collection. Blood and tissue samples were collected immediately post-euthanasia, with serum isolated by centrifugation (3000 ×g, 15 min) and stored at –80 °C until analysis. All experimental procedures involving animals were approved by the Institutional Animal Care and Use Committee of Nanjing Medical University (Approval number: IACUC-1802007) and conducted in compliance with national and institutional ethical standards.

2.2 Measurement of Serum MDA Level

Serum malondialdehyde (MDA) levels, a marker of lipid peroxidation, were quantified using a commercial thiobarbituric acid reactive substances (TBARS) assay kit (#A003-1; Nanjing Jiancheng Bioengineering Institute, Nanjing, China), according to the manufacturer's instructions. Briefly, serum samples were mixed with reagents and incubated at 95 °C for 40 minutes. Absorbance was measured at 532 nm using a microplate spectrophotometer (Multiskan FC model, version 1.0 firmware; Thermo Fisher Scientific, Waltham, MA, USA). MDA concentrations were calculated based on a standard curve and normalized to total protein content.

2.3 Intracellular ROS Analysis

ROS levels were measured in unfractionated total bone marrow cells prepared as a single-cell suspension that were flushed out from femurs of 8-momth-old WT, *Cyp27b1*$^{+/-}$, *Cyp27b1*$^{+/-}$+NAC, *Cyp27b1*$^{+/-}$+$1,25(OH)_2D_3$ mice, by flow cytometry (Becton Dickinson, Heidelberg, Germany) based on fluorescence intensity measurements, as described previously [21].

2.4 Radiography and Micro-Computed Tomography (Micro-CT)

Lumbar spine specimens from 8-month-old WT and *Cyp27b1*$^{+/-}$ mice were harvested and fixed in PLP fixative for 24 hours. Fixed samples were rinsed in PBS and scanned using X-ray radiography (Faxitron Bioptics, Tucson, AZ, USA) and micro-computed tomography (SkyScan 1276 model, Scan software version 1.18; Bruker MicroCT, Kontich, Antwerp, Belgium). Scanning parameters were set at 50 kV, 200 µA, and 9-µm voxel resolution. Three-dimensional reconstruction and quantitative analysis—including bone volume fraction (BV/TV), trabecular thickness (Tb.Th), trabecular number (Tb.N), and trabecular separation (Tb.Sp)—were performed using CTAn software (Bruker). Analyses followed standardized guidelines for bone microarchitecture assessment [22,23].

Table 1. Primers used for real time RT-PCR in this study.

Name	S/AS	Sequence (5′ to 3′)	Tm (°C)	bp
SOD1	S	ATTACAGGATTAACTGAAGG	50	238
	AS	CAATGATGGAATGCTCTC		
Nrf2	S	ACCAAGGGGCACCATATAAAAG	60	114
	AS	CTTCGCCGAGTTGCACTCA		
Nqo1	S	AGGATGGGAGGTACTCGAATC	59	144
	AS	AGGCGTCCTTCCTTATATGCTA		
GSR	S	GACACCTCTTCCTTCGACTACC	60	116
	AS	CCCAGCTTGTGACTCTCCAC		
Hmox1	S	AAGCCGAGAATGCTGAGTTCA	60	100
	AS	GCCGTGTAGATATGGTACAAGGA		
Txnrd1	S	CCCACTTGCCCCAACTGTT	60	134
	AS	GGGAGTGTCTTGGAGGGAC		
CAT	S	GCAGATACCTGTGAACTGTCCCT	60	472
	AS	TTACAGGTTAGCTTTTCCCTTCG		
p16	S	AACTCTTTCGGTCGTACCCC	62	364
	AS	GCGTGCTTGAGCTGAAGCTA		
p21	S	CAATCCTGGTGATGTCCGACCTGTT	70	369
	AS	GAATCTTCAGGCCGCTCAGACACCA		
Bmi1	S	ATCCCCACTTAATGTGTGTCCT	61	116
	AS	CTTGCTGGTCTCCAAGTAACG		
TNFα	S	CCTGTAGCCCACGTCGTAG	62	148
	AS	GGGAGTAGACAAGGTACAACCC		
IL6	S	TAGTCCTTCCTACCCCAATTTCC	61	76
	AS	TTGGTCCTTAGCCACTCCTTC		
ALP	S	CTTGCTGGTGGAAGGAGGCAGG	55	393
	AS	GGAGCACAGGAAGTTGGGAC		
Col-I	S	TCTCCACTCTTCTAGTTCCT	55	269
	AS	TTGGGTCATTTCCACATGC		
OPG	S	TGGAGATCGAATTCTGCTTG	57	719
	AS	TCAAGTGCTTGAGGGCATAC		
Runx2	S	GTGACACCGTGTCAGCAAAG	55	356
	AS	GGAGCACAGGAAGTTGGGAC		
Osterix	S	ATGGCGTCCTCTCTGCTTG	62	156
	AS	TGAAAGGTCAGCGTATGGCTT		
OCN	S	CAAGTCCCACACAGCAGCTT	55	370
	AS	AAAGCCGAGCTGCCAGAGTT		
BSP	S	AGCAAGAAACTCTTCCAAGCAA	60	134
	AS	GTGAGATTCGTCAGATTCATCCG		
M-csf	S	GGCCTTGGAAGCATGTAGAGG	62	104
	AS	GGAGAACTCGTTAGAGACGACTT		
RANKL	S	GGTCGGGCAATTCTGAATT	57	813
	AS	GGGGAATTACAAAGTGCACCAG		
Trap	S	ACACAGTGATGCTGTGTGGCAACTC	57	466
	AS	CCAGAGGCTTCCACATATATGATGG		
CTSK	S	GAAGAAGACTCACCAGAAGCAG	60	102
	AS	TCCAGGTTATGGGCAGAGATT		
c-FMS	S	GGCTTGGCTTGGGATGATTCT	62	126
	AS	GAGGGTCTGGCAGGTACTC		
CTR	S	GCAACGCTTTCACTTCTGAGA	62	297
	AS	GTTCCCACTGCATTGTCCACA		
Nfatc-1	S	GGAGCGGAGAAACTTTGCG	61	94
	AS	GTGACACTAGGGGACACATAACT		

Table 1. Continued.

Name	S/AS	Sequence (5′ to 3′)	Tm (°C)	bp
Mmp13	S	CTTCTTCTTGTTGAGCTGGACTC	62	173
	AS	CTGTGGAGGTCACTGTAGACT		
IL-1α	S	CGAAGACTACAGTTCTGCCATT	60	126
	AS	GACGTTTCAGAGGTTCTCAGAG		
IL-1β	S	GCAACTGTTCCTGAACTCAACT	61	89
	AS	ATCTTTTGGGGTCCGTCAACT		
GAPDH	S	TGGATTTGGACGCATTGGTC	55	211
	AS	TTTGCACTGGTACGTGTTGAT		

bp, base pairs; Tm, Melting temperature; S, Sense; AS, Anti-sense; SOD1, superoxide dismutase 1; Nrf2, nuclear factor erythroid 2-related factor 2; Nqo1, NAD(P)H quinone dehydrogenase 1; GSR, glutathione reductase; Hmox1, heme oxygenase 1; Txnrd1, thioredoxin reductase 1; CAT, catalase; Bmi1, B lymphoma Mo-MLV insertion region 1 homolog; TNFα, tumor necrosis factor alpha; IL6, interleukin 6; ALP, alkaline phosphatase; Col-I, type 1 collagen; OPG, osteoprotegerin; Runx2, Runt-related transcription factor 2; OCN, osteocalcin; BSP, bone sialoprotein; M-csf, macrophage colony-stimulating factor; RANKL, receptor activator of nuclear factor kappa-B ligand; CTSK, cathepsin K; c-FMS, colony-stimulating factor 1 receptor; CTR, calcitonin receptor; Nfatc-1, nuclear factor of activated T-cells, cytoplasmic 1; Mmp13, matrix metallopeptidase 13; GAPDH, glyceraldehyde-3-phosphate dehydrogenase; RT-PCR, reverse transcription polymerase chain reaction.

2.5 Histology, Histochemistry, and Immunohistochemistry

Vertebral bone specimens were decalcified in 10% EDTA (pH 7.4) for 2–3 weeks, processed through graded alcohols, embedded in paraffin, and sectioned at 5-µm thickness. Tissue sections were stained with hematoxylin and eosin (H&E) for general histology, histochemically for total collagen, naphthol AS-MX phosphate with fast Red TR for alkaline phosphatase (ALP) activity to identify osteoblasts, followed by counterstaining with Vector methyl green as a nuclear counterstain [24], and naphthol AS-BI phosphate with fast red violet LB for tartrate-resistant acid phosphatase (TRAP) to identify osteoclasts. For immunohistochemistry, antigen retrieval was performed using citrate buffer (pH 6.0) under heat-induced conditions. Sections were blocked with 5% normal goat serum and incubated overnight at 4 °C with primary antibodies against superoxide dismutase 1 (SOD1; catalog no. ab16831, lot #GR123456, dilution 1:200; Abcam, Cambridge, UK), 8-hydroxy-2′-deoxyguanosine (8-OHdG; catalog no. ab48508, lot #GR234567, dilution 1:100; Abcam, Cambridge, UK), and β-galactosidase (β-gal; catalog no. ab203749, lot #GR345678, dilution 1:200; Abcam, Cambridge, UK). Detection was performed using horseradish peroxidase (HRP)-conjugated secondary antibodies (goat anti-rabbit IgG-HRP, catalog no. ab205718, lot #GR456789, dilution 1:500; Abcam, Cambridge, UK; or goat anti-mouse IgG-HRP, catalog no. ab214879, lot #GR567890, dilution 1:500; Abcam, Cambridge, UK) and 3,3′-diaminobenzidine chromogen (DAB substrate kit, catalog no. ab64238, lot #GR678901; Abcam, Cambridge, UK). Nuclei were counterstained with hematoxylin. Slides were imaged using a Leica DM2500 microscope, and positive staining was quantified using ImageJ with threshold-based analysis.

2.6 Western Blots

Proteins were extracted from vertebral bone tissues using RIPA lysis buffer supplemented with protease and phosphatase inhibitors (Roche). Lysates were homogenized, centrifuged (12,000 ×g, 15 min, 4 °C), and protein concentrations determined by BCA assay. Equal amounts of protein (30–50 µg) were separated by SDS-PAGE and transferred to PVDF membranes. Membranes were blocked with 5% non-fat milk in TBST and incubated overnight at 4 °C with the following primary antibodies: anti-Nrf2 (catalog no. BS1258, lot #A12345, dilution 1:1000; Bioworld Technology, Inc., Dublin, OH, USA), anti-Sod1 (catalog no. ab13498, lot #GR345678, dilution 1:1000; Abcam, Cambridge, UK), anti-γH2AX (catalog no. ab11174, lot #GR456789, dilution 1:1000; Abcam, Cambridge, UK), anti-CDK4 (catalog no. ab108357, lot #GR567890, dilution 1:1000; Abcam, Cambridge, UK), anti-CDK6 (catalog no. 3136, lot #25, dilution 1:1000; Cell Signaling Technology, Danvers, MA, USA), anti-p16 (catalog no. ab108349, lot #GR678901, dilution 1:1000; Abcam, Cambridge, UK), anti-p21 (catalog no. sc-6246, lot #B0123, dilution 1:500; Santa Cruz Biotechnology, Dallas, TX, USA), anti-p53 (catalog no. sc-126, lot #C0345, dilution 1:500; Santa Cruz Biotechnology, Dallas, TX, USA), anti-Cyclin D1 (catalog no. ab134175, lot #GR789012, dilution 1:1000; Abcam, Cambridge, UK), anti-Bmi1 (catalog no. 05-637, lot #DAM123456, dilution 1:1000; MilliporeSigma, Burlington, MA, USA), and anti-β-actin (catalog no. AP0060, lot #B23456, dilution 1:2000; Bioworld Technology, Inc.,

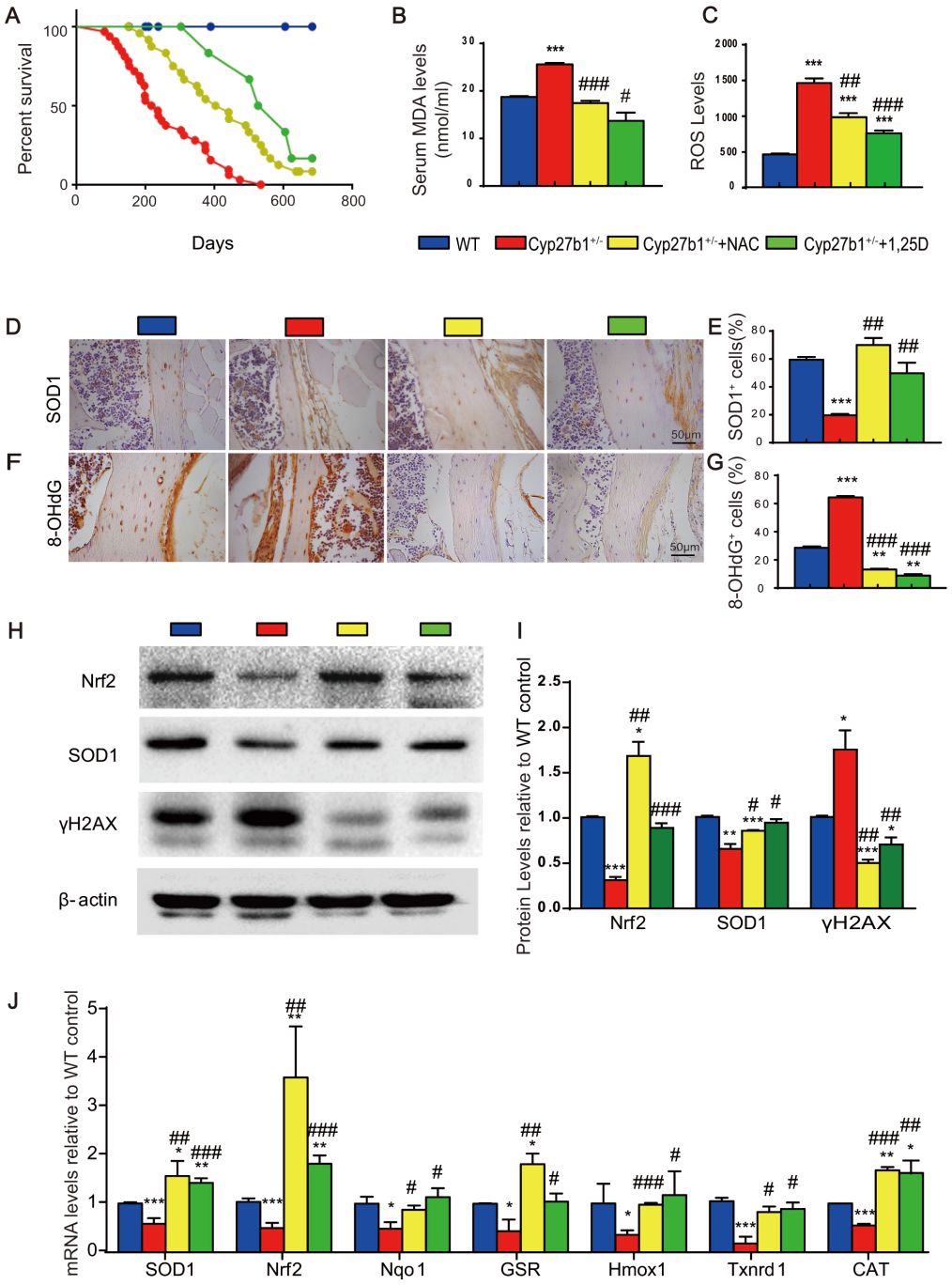

Fig. 1. NAC or exogenous 1,25(OH)$_2$D$_3$ extends lifespan and suppresses oxidative stress and DNA damage in *Cyp27b1*$^{+/-}$ mice. (A) Kaplan–Meier survival curves for WT, *Cyp27b1*$^{+/-}$, and *Cyp27b1*$^{+/-}$ mice supplemented with NAC or 1,25(OH)$_2$D$_3$ on a standard diet; groups compared by log-rank test. (B) Serum malondialdehyde (MDA) concentrations reflecting systemic lipid peroxidation in 8month-old mice. (C) Reactive oxygen species (ROS) levels in bone marrow cells. (D) Immunohistochemistry for SOD1-positive cells in vertebral sections (Scale bar = 50 μm) and (E) quantification of positive area. (F) Immunohistochemistry (Scale bar = 50 μm) and (G) quantification for 8-OHdG-positive cells indicating oxidative DNA damage. (H,I) Representative Western blots and quantification of Nrf2, SOD1, and γH2AX protein. (J) Relative mRNA expression of antioxidant genes. Data are mean ± S.E.M. (n = 5 per group). Significance: * $p < 0.05$, ** $p < 0.01$, *** $p < 0.001$ vs WT; # $p < 0.05$, ## $p < 0.01$, ### $p < 0.001$ vs Cyp27b1$^{+/-}$. NAC, N-acetylcysteine; WT, wild-type; SOD1, superoxide dismutase 1; Nrf2, nuclear factor erythroid 2-related factor 2; γH2AX, gamma-H2AX; S.E.M, standard error of the mean.

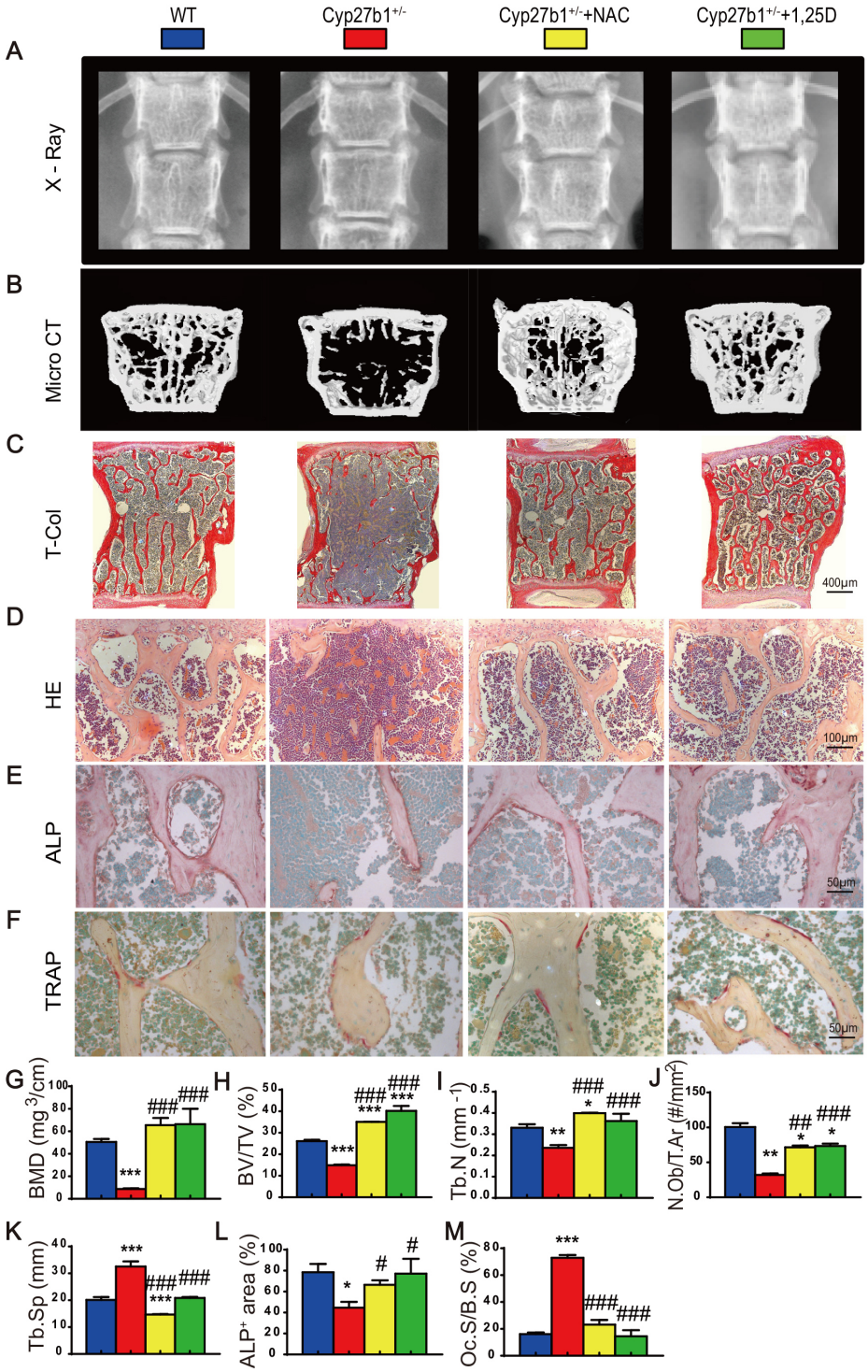

Fig. 2. NAC or exogenous $1,25(OH)_2D_3$ ameliorates bone loss due to Cyp27b1 haploinsufficiency. (A) Lumbar spine Xrays. (B) MicroCT scans and 3D reconstructions of lumbar vertebrae. (C) Total collagen staining of vertebral sections (Scale bar = 400 μm). (D) Hematoxylin and eosin (H&E) staining (Scale bar = 100 μm). (E) Alkaline phosphatase (ALP) staining (Scale bar = 50 μm). (F) Tartrate-resistant acid phosphatase (TRAP) staining (Scale bar = 50 μm). (G) Bone mineral density (BMD, mg/cm^3). (H) Trabecular bone volume fraction (BV/TV, %). (I) Trabecular number (Tb.N, #/mm). (J) Osteoblast number (N.Ob/T.Ar, #/mm^2). (K) Trabecular separation (Tb.Sp, μm). (L) ALP-positive area (%). (M) Osteoclast surface (Oc.S/B.S, %). Data are mean ± S.E.M. (n = 5). Significance: * $p < 0.05$, ** $p < 0.01$, *** $p < 0.001$ vs WT; # $p < 0.05$, ## $p < 0.01$, ### $p < 0.001$ vs Cyp27b1$^{+/-}$.

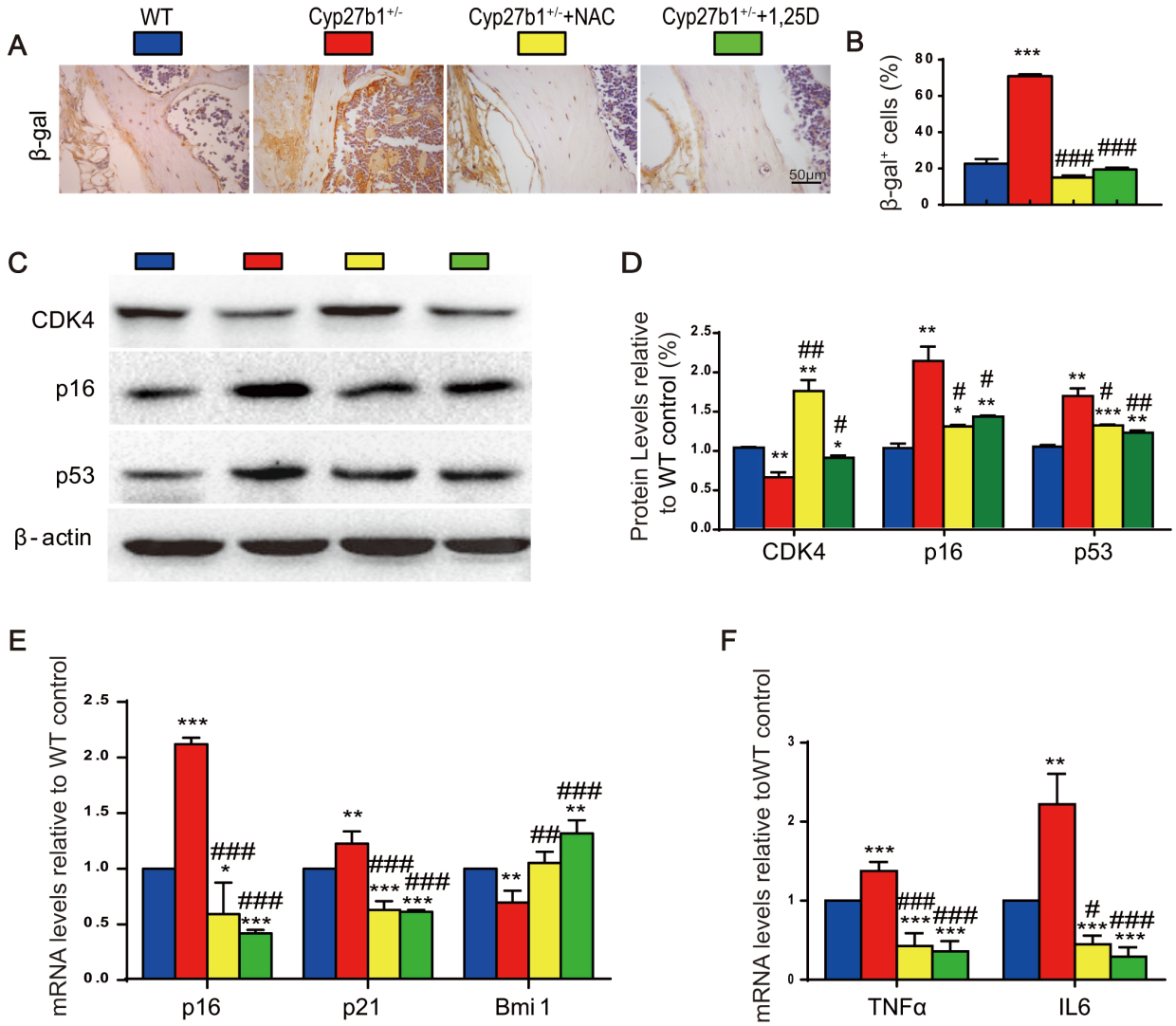

Fig. 3. NAC or exogenous 1,25(OH)$_2$D$_3$ delays skeletal aging caused by Cyp27b1 haploinsufficiency. (A) β-galactosidase (β-gal) staining in vertebral sections (Scale bar = 50 µm). (B) Quantification of β-gal-positive area (%). (C,D) Western blots and quantification of p16, p53, and CDK4 normalized to loading control. (E) Relative mRNA levels of *p16*, *p21*, and *Bmi1*. (F) Relative mRNA levels of SASP factors *TNFα* and *IL6*. Data are mean ± S.E.M. (n = 5 per group). Significance: * $p < 0.05$, ** $p < 0.01$, *** $p < 0.001$ vs WT; # $p < 0.05$, ## $p < 0.01$, ### $p < 0.001$ vs *Cyp27b1*$^{+/-}$. CDK4, cyclin-dependent kinase 4; *Bmi1*, B lymphoma Mo-MLV insertion region 1 homolog; SASP, senescence-associated secretory phenotype; *TNFα*, tumor necrosis factor alpha; *IL6*, interleukin 6.

Dublin, OH, USA). HRP-conjugated secondary antibodies (dilution 1:5000; Cell Signaling Technology, Danvers, MA, USA; anti-rabbit IgG HRP catalog no. 7074, lot #28; anti-mouse IgG HRP catalog no. 7076, lot #29) were applied for 1 hour at room temperature. Protein bands were visualized using enhanced chemiluminescence (ECL, catalog no. 1705061, lot #L012345; Bio-Rad Laboratories, Hercules, CA, USA) and imaged with a ChemiDoc XRS+ system (version 6.1 software; Bio-Rad Laboratories, Hercules, CA, USA). Band intensities were quantified using ImageJ software (version 1.53; National Institutes of Health, Bethesda, MD, USA) and normalized to β-actin.

2.7 RNA Extraction and Real-Time RT-PCR

Total RNA was extracted from vertebral bone tissue using Trizol Reagent (Invitrogen) according to the manufacturer's protocol. RNA concentration and purity were assessed by spectrophotometry (A260/A280 ratio >1.8). cDNA was synthesized from 1 µg of total RNA using PrimeScript RT Master Mix (catalog no. RR036A, lot #AK12345; TaKaRa Bio Inc., Kusatsu, Shiga, Japan). Real-time quantitative PCR was performed using a Agilent AriaMx Real-Time PCR System with SYBR Green Master Mix (catalog no. RR820A, lot #AL23456; TaKaRa Bio Inc., Kusatsu, Shiga, Japan). Amplification conditions included an initial denaturation at 95 °C for 30 s,

followed by 40 cycles of 95 °C for 5 s and 60 °C for 30 s. Target gene expression was normalized to the housekeeping gene glyceraldehyde-3-phosphate dehydrogenase (*GAPDH*). Relative expression levels were calculated using the $2^{-\Delta\Delta Ct}$ method. Primer sequences are listed in Table 1.

2.8 Statistics

All data are presented as mean ± standard error of the mean (SEM), and were derived from at least three independent biological replicates. To ensure adequate statistical power and reliability, particularly for multi-group comparisons and lifespan analyses, a sample size of n = 5–6 mice per group was selected based on prior pilot studies and effect size estimates from similar experimental models in the literature. This sample size provides sufficient power (>80%) to detect biologically meaningful differences with an alpha level of 0.05, assuming a moderate to large effect size, which is consistent with the robust phenotypic changes observed in our study. Data were analyzed using GraphPad Prism (version 9.0). Comparisons between two groups were performed using an unpaired Student's *t*-test, while multi-group comparisons were conducted by two-way analysis of variance (ANOVA) followed by Tukey's or Sidak's post hoc tests, as appropriate. Survival analyses were performed using the log-rank (Mantel-Cox) test. Statistical significance was defined as $p < 0.05$.

3. Results

3.1 Role of the Antioxidant NAC or of Exogenous Active Vitamin D in Extending Lifespan and Suppressing Oxidative Stress and DNA Damage in Cyp27b1$^{+/-}$ Mice

To determine whether active vitamin D delays aging by suppressing oxidative stress and DNA damage, male *Cyp27b1*$^{+/-}$ mice were given either the antioxidant N-acetylcysteine (NAC) in drinking water from 3 weeks of age after weaning, or 1,25(OH)$_2$D$_3$ by subcutaneous injection. Age-matched WT and *Cyp27b1*$^{+/-}$ males on a standard diet served as controls. Survival was monitored across groups. In 8-month-old mice, serum MDA was measured biochemically; ROS levels in bone marrow cells were quantified by 2′,7′-Dichlorofluorescin diacetate (DCF-DA) staining and flow cytometry; and DNA damage and antioxidant markers in bone were assessed by immunohistochemistry, Western blots, and real-time RT–PCR.

Cyp27b1$^{+/-}$ mice on a standard diet had a mean lifespan of 241 days (range 80–534), which was extended to 398 days (182–636) by NAC and to 583 days (382–700) by 1,25(OH)$_2$D$_3$ (Fig. 1A). Relative to WT controls, 8-month-old *Cyp27b1*$^{+/-}$ mice exhibited significantly elevated serum MDA and bone ROS, both of which were reduced by NAC or 1,25(OH)$_2$D$_3$ supplementation (Fig. 1B,C). In vertebrae from Cyp27b1$^{+/-}$ mice, the proportion of SOD1-positive cells (Fig. 1D,E), SOD1 and Nrf2 protein levels (Fig. 1H,I), and mRNA levels of Nrf2 target genes (*Nqo1*, *Gsr*, *Hmox1*, *Txnrd1*, and *Cat*; Fig. 1J) were all decreased, while DNA damage markers—8OHdG-positive cells (Fig. 1F,G) and γH2AX protein (Fig. 1H,I)—were increased. NAC or exogenous 1,25(OH)$_2$D$_3$ significantly corrected the downregulation of antioxidant enzymes and the elevations in DNA damage markers (Fig. 1B–J). These findings indicate that active vitamin D effectively delays aging and suppresses oxidative stress and DNA damage in bone by maintaining redox homeostasis.

3.2 NAC or Exogenous 1,25(OH)$_2$D$_3$ Prevents Bone Loss Caused by Active Vitamin D Haploinsufficiency

To test whether NAC or 1,25(OH)$_2$D$_3$ can rescue bone loss induced by active vitamin D haploinsufficiency, we analyzed vertebral phenotypes in the four groups of 8-month-old mice by imaging and histology. Compared with WT, *Cyp27b1*$^{+/-}$ mice showed significant reductions in vertebral bone mineral density (BMD), bone volume, trabecular number and thickness, total collagen-stained area, and osteoblasts with reduced ALP-positive area; in addition, there was increased trabecular separation and greater TRAP-positive osteoclast surface (Fig. 2A–M). NAC or 1,25(OH)$_2$D$_3$ supplementation markedly improved these parameters, reversing bone loss, low BMD, trabecular architectural deterioration, collagen reduction, osteoblast depletion, and osteoclast expansion (Fig. 2A–M). These results suggest that active vitamin D counters osteoporosis by limiting oxidative stress, thereby promoting osteoblast-mediated bone formation and restraining osteoclast-mediated bone resorption.

3.3 NAC or Exogenous 1,25(OH)$_2$D$_3$ Delays Skeletal Aging Driven by Active Vitamin D Haploinsufficiency

To evaluate skeletal aging, senescence-associated markers were examined in vertebrae from the four groups of 8-month-old mice using immunohistochemistry, Western blots, and real-time RT–PCR. Relative to WT, *Cyp27b1*$^{+/-}$ mice showed increased βgalactosidase (β-gal) staining (Fig. 3A,B), elevated p16 and p53 protein (Fig. 3C,D), higher mRNA levels of *p16* and *p21* (Fig. 3E), and increased SASP cytokines *TNFα* and *IL6* (Fig. 3F). Conversely, CDK4 protein (Fig. 3C,D) and *Bmi1* mRNA (Fig. 3E) were reduced. NAC or 1,25(OH)$_2$D$_3$ significantly ameliorated these senescence and SASP abnormalities. Thus, active vitamin D effectively delays skeletal aging by suppressing cellular senescence and SASP.

3.4 p16 Deletion Rescues Bone Loss Caused by Active Vitamin D Haploinsufficiency

Given the robust upregulation of p16 in bone, we generated double-mutant mice lacking p16 on a *Cyp27b1*$^{+/-}$ background (*p16*$^{-/-}$*Cyp27b1*$^{+/-}$), and compared their skeletal phenotypes at 8 months on a standard diet, with *WT*, *p16*$^{-/-}$, and *Cyp27b1*$^{+/-}$ littermates. Imaging and histology showed that, relative to *WT*, *Cyp27b1*$^{+/-}$ mice had significantly reduced BMD, bone volume, and trabecular num-

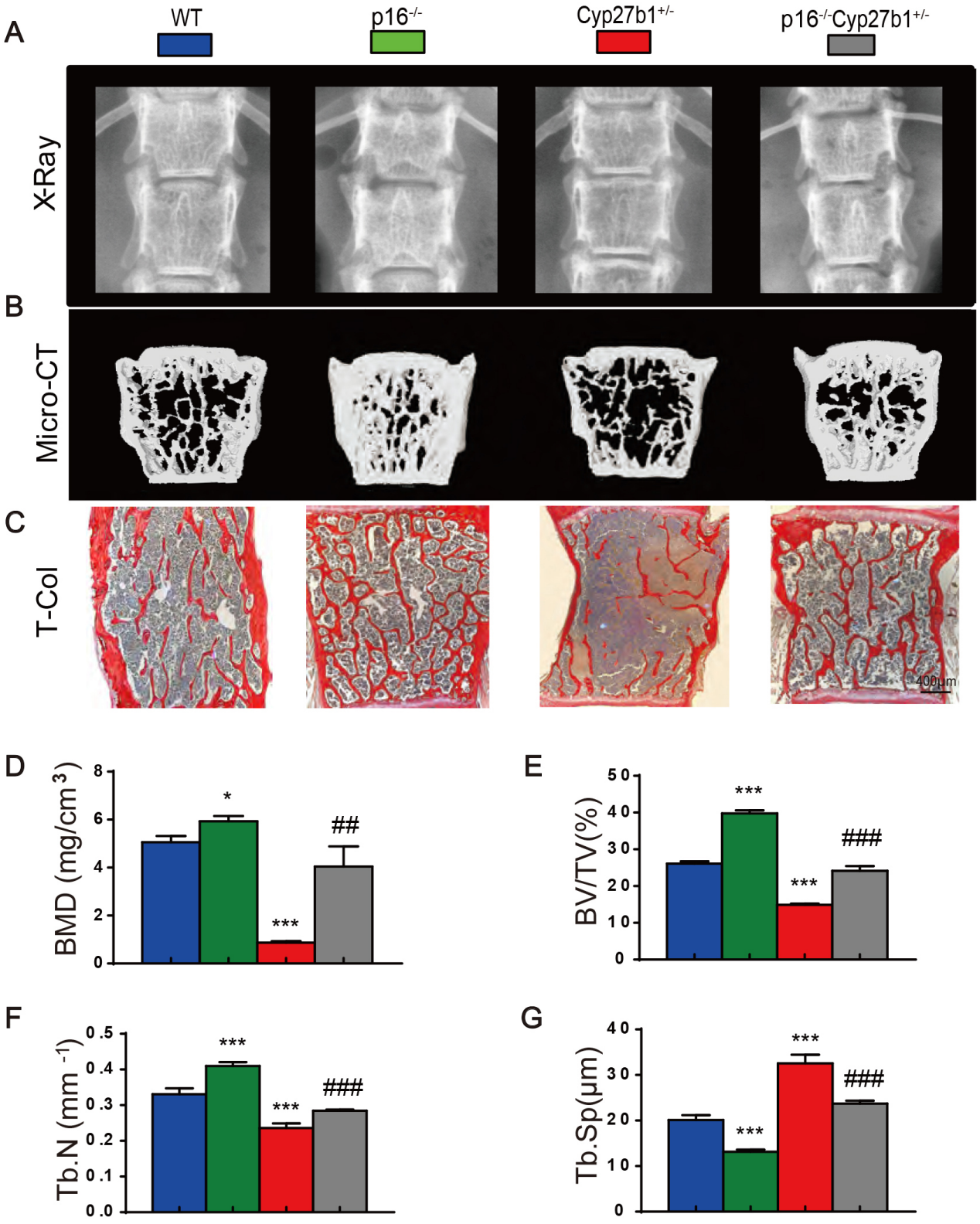

Fig. 4. p16 deletion mitigates bone loss due to Cyp27b1 haploinsufficiency. (A) Lumbar spine Xrays. (B) MicroCT and 3D reconstructions. (C) Total collagen staining of vertebral sections (Scale bar = 400 μm). (D) Bone mineral density (BMD, mg/cm^3). (E) Trabecular bone volume fraction (BV/TV, %). (F) Trabecular number (Tb.N, #/mm). (G) Trabecular separation (Tb.Sp, μm). Data are mean ± S.E.M. (n = 5 per group). Significance: * $p < 0.05$, *** $p < 0.001$ vs WT; ## $p < 0.01$, ### $p < 0.001$ vs *Cyp27b1*$^{+/-}$.

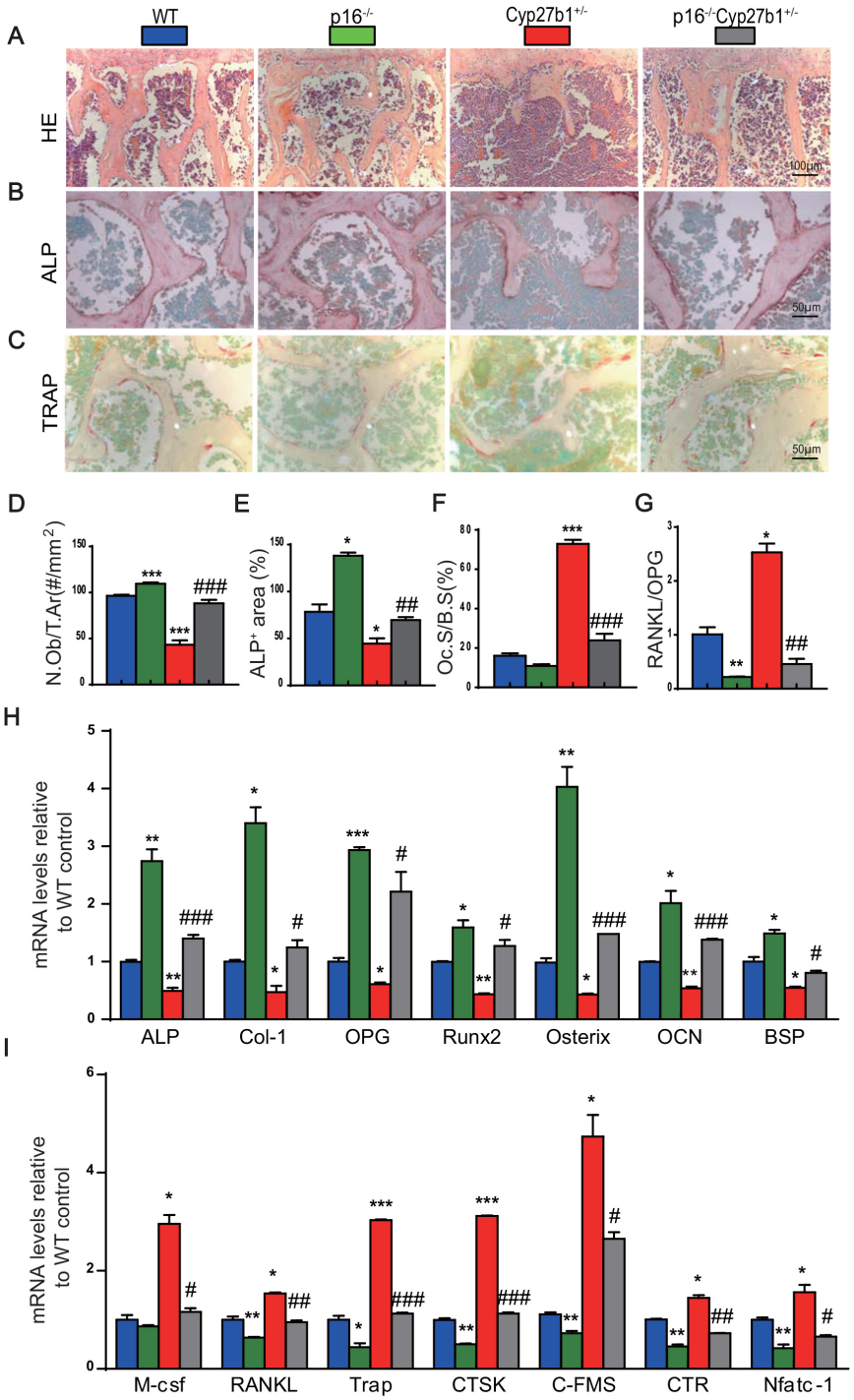

Fig. 5. p16 deletion corrects the reduced bone formation and the increased bone resorption in Cyp27b1 haploinsufficiency. (A) H&E staining (Scale bar = 100 μm). (B) ALP staining (Scale bar = 50 μm). (C) TRAP staining of vertebral trabeculae (Scale bar = 50 μm). (D) Osteoblast number per trabecular area (N.Ob/T.Ar, #/mm^2). (E) ALP-positive area (%). (F) Osteoclast surface per bone surface (Oc.S/B.S, %). (G) *RANKL*/*OPG* mRNA ratio in vertebral bone. (H) Relative mRNA levels of osteogenic marker genes, including alkaline phosphatase (*ALP*), collagen type I (*Col I*), osteoprotegerin (*OPG*), Runt-related transcription factor 2 (*Runx2*), osterix (*OSX*), osteocalcin (*OCN*), and bone sialoprotein (*BSP*). (I) Relative mRNA levels of osteoclastic marker genes, including macrophage colony-stimulating factor (*M-csf*), receptor activator of nuclear factor kappa-B ligand (*RANKL*), tartrate-resistant acid phosphatase (*TRAP*), cathepsin K (*CTSK*), colony-stimulating factor 1 receptor (*c-FMS*), calcitonin receptor (*CTR*), and nuclear factor of activated T cells cytoplasmic 1 (*Nfatc1*). Data are mean ± S.E.M. (n = 5 per group). Significance: * $p < 0.05$, ** $p < 0.01$, *** $p < 0.001$ vs WT; # $p < 0.05$, ## $p < 0.01$, ### $p < 0.001$ vs Cyp27b1$^{+/-}$.

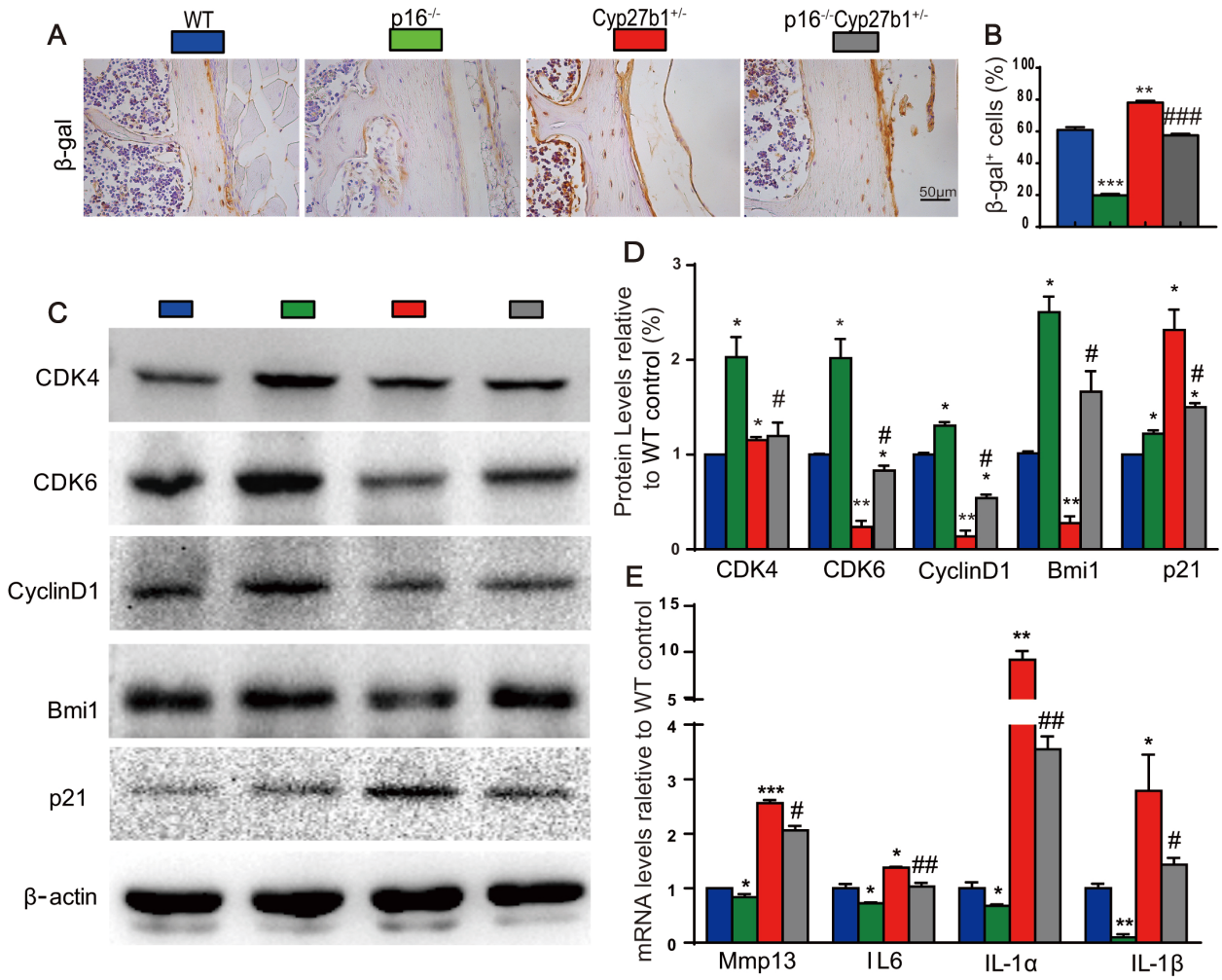

Fig. 6. p16 deletion suppresses skeletal cell senescence induced by Cyp27b1 haploinsufficiency. (A) β-gal staining in vertebral sections (Scale bar = 50 μm). (B) Quantification of β-gal-positive area (%). (C,D) Western blots and quantification of CDK4, CDK6, Cyclin D1, Bmi1, and p21 normalized to loading control. (E) Relative mRNA levels of SASP factors (*IL6*, *MMP13*, *IL1α*, *IL1β*) normalized to Gapdh. Data are mean ± S.E.M. (n = 5 per group). Significance: * $p < 0.05$, ** $p < 0.01$, *** $p < 0.001$ vs WT; # $p < 0.05$, ## $p < 0.01$, ### $p < 0.001$ vs *Cyp27b1*$^{+/-}$.

ber and thickness, along with increased trabecular separation (Fig. 4A–G). Strikingly, p16 deletion in *Cyp27b1*$^{+/-}$ mice restored bone mass, BMD, and trabecular number and thickness, and reduced trabecular separation (Fig. 4A–G). These data demonstrate that p16 loss effectively corrects bone loss resulting from active vitamin D haploinsufficiency.

3.5 p16 Deletion Corrects Reduced Bone Formation and Increased Bone Resorption

To determine whether p16 deletion ameliorates impaired bone formation and excessive resorption, we assessed osteogenic and osteoclastic indices in vertebrae from the four genotypes at 8 months. Compared with *WT*, *p16*$^{-/-}$ mice exhibited increased osteoblast numbers and ALP-positive area, with higher mRNA levels of osteogenic genes (*ALP*, *ColI*, osteoprotegerin (*OPG*), Runt-related transcription factor 2 (*Runx2*), *Osterix*, osteocalcin (*OCN*), and bone sialoprotein (*BSP*)). In contrast, Cyp27b1$^{+/-}$ mice had reduced osteoblast numbers and ALP-positive area, and downregulated osteogenic gene expression. Notably, p16 deletion in *Cyp27b1*$^{+/-}$ mice increased osteoblast numbers and ALP-positive area and upregulated osteogenic genes (Fig. 5A,B,D,E,H). On the resorptive side, *Cyp27b1*$^{+/-}$ mice displayed increased TRAP-positive osteoclast surface, an elevated receptor activator of nuclear factor kappa-B ligand (*RANKL*)/*OPG* mRNA ratio, and higher mRNA levels of resorption-associated genes (*Mcsf*, *RANKL*, *TRAP*, *CTSK*, *cFMS*, *CTR*, and *Nfatc1*). p16 deletion in *Cyp27b1*$^{+/-}$ mice reduced osteoclast surface and downregulated these resorptive genes (Fig. 5C,F,G,I). Thus, p16 loss rescues vitamin D haploinsufficiency–induced bone loss by promoting formation and inhibiting resorption.

3.6 p16 Deletion Suppresses Skeletal Cell Senescence and SASP Induced by Active Vitamin D Haploinsufficiency

We next examined whether p16 deletion mitigates skeletal cell senescence and SASP. Relative to WT, *Cyp27b1*$^{+/-}$ mice exhibited increased β-gal staining and p21 protein (Fig. 6A–D), reduced expression of cell-cycle regulators (CDK4, CDK6, Cyclin D1, and Bmi1, Fig. 6C,D), and elevated mRNA levels of SASP factors (*IL6*, *Mmp13*, *IL1*α, and *IL1*β). In *p16*$^{-/-}$*Cyp27b1*$^{+/-}$ mice, β-gal and p21 were reduced, SASP gene expression was decreased, and CDK4, CDK6, Cyclin D1, and Bmi1 protein levels were increased (Fig. 6A–E). These data indicate that p16 deletion exerts anti-osteoporotic effects by suppressing skeletal cell senescence and SASP.

4. Discussion

Our findings define a vitamin D–redox–senescence axis that governs skeletal remodeling during aging by linking active vitamin D insufficiency to heightened ROS, attenuated Nrf2/SOD1 defenses, and increased DNA damage, culminating in p53–p21 and p16 activation, SASP induction, suppressed osteoblastogenesis, elevated osteoclast activity, and trabecular deterioration [3,5,12,25]. Both NAC and 1,25(OH)$_2$D$_3$ reversed these molecular and cellular abnormalities, and genetic attenuation of p16 restored bone mass by enhancing formation and reducing resorption while dampening SASP, underscoring senescence as a causal node in this pathway [4]. Mechanistically, our data support a model in which sufficient 1,25(OH)$_2$D$_3$ constrains oxidative and genotoxic stress to prevent sustained activation of senescence checkpoints and pro-osteoclastogenic SASP factors that impair osteoblast lineage commitment and promote osteoclastogenesis [3–5,12,25]. These results are consistent with literature linking ROS and DDR signaling to bone aging and demonstrating that bolstering antioxidant defenses curtails osteoclastogenesis and preserves osteoblast function [26–30]. They also converge with reports that VDR signaling interfaces with chromatin and cell-cycle regulators (for example, EZH2–p16) to restrain senescence programs in bone [31,32]. At the tissue level, NAC and 1,25(OH)$_2$D$_3$ improved osteoblast indices, collagen deposition, and microarchitecture while reducing osteoclast surface, in line with studies showing that mitigating oxidative stress shifts the formation–resorption balance toward anabolism and that perturbation of redox sensors such as Nrf2 alters this balance [28–30,33]. The reduction in osteoclast surface, together with vitamin D/VDR modulation of osteoclastogenic mediators, provides a plausible mechanism for antiresorptive benefit in aging bone [34,35]. Collectively, these data highlight redox–senescence signaling as a tractable therapeutic target and suggest that maintaining sufficient active vitamin D or pharmacologically buffering ROS may mitigate skeletal aging by limiting p16-driven chronic senescence.

In parallel, in WT cohorts, long-term NAC (1 mg/mL in drinking water) and 1,25(OH)$_2$D$_3$ (0.1 µg/kg, s.c.) did not alter survival compared with untreated WT controls up to at least 600 days of age, indicating no lifespan extension under these regimens. Consistent with prior literature, neither intervention produced adverse skeletal phenotypes; NAC modestly improved redox status with trends toward preservation of age-sensitive trabecular microarchitecture [36], while 1,25(OH)$_2$D$_3$ maintained calcium homeostasis and attenuated age-related declines in bone formation indices, accompanied by activation of Nrf2- and VDR-dependent signaling [18]. These observations align with established evidence that vitamin D signaling mitigates skeletal aging and that antioxidant modulation of ROS can temper senescence-associated bone deterioration [37], providing contextual support for our mechanistic findings while explaining the omission of detailed WT control data from the main text.

It is important to acknowledge the inherent complexities of skeletal aging and to interpret our findings within this broader biological context. While the antioxidant NAC effectively rescued the bone phenotype in our model, supporting a key role for oxidative stress, its broad mechanism of action means that its benefits may extend beyond the direct quenching of reactive oxygen species to influence other redox-sensitive signaling pathways [38]. Likewise, while genetic deletion of *p16*^{Ink4a} provides strong evidence for its role as a key effector in this process, this intervention may have pleiotropic effects. Cellular senescence is a fundamentally bivalent process, with beneficial roles in tumor suppression and tissue repair that may be compromised by its systemic elimination [3,4]. The long-term consequences of constitutive p16 deletion, including potential impacts on cancer incidence or wound healing, were not assessed in this study and represent an important area for future investigation [26]. Therefore, the vitamin D–redox–senescence axis identified here should be viewed as a critical contributor to skeletal aging, which likely interacts with other well-established regulators such as hormonal fluctuations, mechanical loading, and systemic inflammation to determine the final bone phenotype.

While both NAC and exogenous 1,25(OH)$_2$D$_3$ significantly rescued vitamin D deficiency-induced phenotypes, our study was not designed for direct therapeutic comparison. Notably, 1,25(OH)$_2$D$_3$ more completely normalized lifespan and senescence markers, suggesting more targeted pathway correction. Beyond its role as a glutathione precursor, NAC's benefits likely involve pleiotropic mechanisms including direct ROS scavenging, NF-κB modulation, and mitochondrial stabilization [39,40]. Importantly, our data do not address toxicity profiles, optimal dosing, or long-term consequences of these interventions—particularly the tumor suppression trade-offs of constitutive p16 deletion [26]. Therefore, we emphasize physiological vitamin D replenishment (targeting 25(OH)D sufficiency) as a first-line

approach supported by clinical guidelines [7], with intermittent active vitamin D regimens considered for targeted applications where hypercalcemia risks can be mitigated through close monitoring [41].

Genetic evidence from p16 deletion strengthens the causal link between senescence and osteopenia in the presence of vitamin D insufficiency. Removing p16 normalized bone mass, increased osteogenic programs, reduced osteoclast surface and RANKL/OPG ratio, and suppressed SASP. This mirrors evidence that targeting senescent cells prevents age-related bone loss and rejuvenates remodeling [26,27] and supports p16 as a key effector coupling redox/genotoxic stress to skeletal aging [31,32,42]. It is important to contextualize the role of the Senescence-Associated Secretory Phenotype (SASP) as both a consequence of cellular stress and a driver of tissue pathology. The SASP is highly heterogeneous, but the components we identified as elevated in the bone of *Cyp27b1*$^{+/-}$ mice—including the pro-inflammatory cytokines TNFα, IL-6, IL-1α, and IL-1β, and the matrix metalloproteinase MMP13—are canonical factors with potent, well-established roles in skeletal remodeling. Specifically, these cytokines are known to robustly promote osteoclast differentiation and activity while inhibiting osteoblast function, thereby directly contributing to a net catabolic state in bone [43,44]. While oxidative stress and DNA damage are the upstream instigators, our findings position the p16/SASP axis as a critical causal mediator rather than a passive bystander. The genetic deletion of p16 in *Cyp27b1*$^{+/-}$ mice not only suppressed the expression of these SASP factors but also rescued the bone loss phenotype entirely. This provides compelling evidence that the establishment of a p16-dependent senescent state, and the chronic paracrine signaling from its associated SASP, is a key mechanistic link between vitamin D insufficiency and the pathological disruption of bone homeostasis [45]. Therefore, the inflammation observed in our model appears to be an integral component of the senescence program, which perpetuates a pro-resorptive microenvironment.

Cellular senescence in bone reflects convergent yet distinct checkpoint programs governed by the p53–p21^{CIP1} and p16^{INK4a}–RB pathways. Acute oxidative stress commonly activates the DNA damage response (DDR), leading to p53 stabilization and transcriptional induction of p21, which enforces an initial, often reversible growth arrest to facilitate repair [5,6,12,46]. In contrast, chronic or unresolvable stressors—including sustained ROS and mitochondrial dysfunction—favor engagement of p16^{INK4a}, promoting a more durable RB-mediated arrest associated with a stable SASP [3,5,6,12,25]. In our model of active vitamin D insufficiency, we observed a rapid increase in p21 coincident with early ROS elevations, consistent with DDR activation, followed by a predominant and persistent upregulation of p16 that correlated with osteopenic remodeling and SASP enrichment. This temporal sequence supports a two-stage paradigm in osteolineage cells: p53–p21 predominates during the initiation phase, whereas p16 maintains long-term senescence and reinforces paracrine dysfunction affecting osteoclastogenesis and osteoblast differentiation [3,5,6,12,25]. Notably, antioxidant intervention attenuated p21 induction and blunted subsequent p16 accumulation, implicating oxidative stress as a shared upstream driver. These findings align with reports that p21-associated arrest can be reversible and less pro-inflammatory, whereas p16-driven senescence is more stable and SASP-potent, thereby exerting stronger deleterious effects on bone turnover [3–6,12,25,47]. Thus, while p16 appears to be the principal mediator of the sustained senescent phenotype underlying skeletal aging in our model, the p53–p21 axis likely acts as an early sentinel whose modulation may determine whether cells recover or transition to p16-dependent chronic senescence.

Beyond bone, lifespan extension with NAC and 1,25(OH)$_2$D$_3$ suggests organismal benefits from mitigating oxidative stress and senescence, echoing reports that senescence modulation extends healthspan and that systemic redox improvements benefit multiple tissues [14,23,26]. Translationally, maintaining vitamin D sufficiency may protect bone by preserving intracellular redox and genomic stability. Antioxidants and senescence-modulating approaches (senolytics/senomorphics) could complement vitamin D repletion in osteoporosis—particularly in vitamin D insufficiency—with careful attention to safety and dosing [14,23,26,28]. Because pharmacologic 1,25(OH)$_2$D$_3$ can cause hypercalcemia, physiological vitamin D repletion and bone-targeted or intermittent regimens for active analogs warrant consideration [34].

Clinical implications emerge on several fronts. First, maintaining adequate vitamin D status may protect bone not only by optimizing calcium–phosphate balance but also by preserving intracellular redox and genomic stability in skeletal cells [4,7,9,18–20,48–50]. Second, antioxidants such as NAC and agents that activate Nrf2 could complement vitamin D repletion to dampen oxidative stress–driven bone aging, though dosing, duration, and offtarget effects require careful evaluation [37,51]. Third, senescence-targeted strategies (senolytics/senomorphics) merit exploration in osteoporosis, particularly when vitamin D insufficiency is present, with attention to safety and tissue specificity [4,14,50]. Because pharmacologic 1,25(OH)$_2$D$_3$ can cause hypercalcemia, translational paths should prioritize physiological vitamin D repletion (cholecalciferol/25OHD) and consider bonetargeted or intermittent regimens for active analogs [7,9,18,48,49,52].

The therapeutic potential of vitamin D in modulating senescence pathways suggests promising avenues for clinical intervention, particularly when combined with emerging senolytic agents. Preclinical evidence, including data presented in this study, indicates that vitamin D receptor activation can suppress senescence-associated secre-

tory phenotype (SASP) and enhance clearance of senescent cells, potentially augmenting the efficacy of senolytics such as dasatinib and quercetin [14]. A combinatorial approach may allow for lower, safer doses of both agents, reducing the risk of adverse effects. However, the use of active vitamin D analogs, such as calcitriol, carries a well-documented risk of hypercalcemia, especially in older adults and individuals with impaired renal function [7]. To mitigate this, strategies including intermittent dosing regimens, close monitoring of serum calcium and parathyroid hormone levels, and patient selection based on vitamin D deficiency status may be employed [41]. Furthermore, the use of less calcemic vitamin D analogs or prodrug formulations currently under investigation could offer a safer profile for long-term use in aging populations [53]. Future clinical trials should evaluate the safety and efficacy of such combination therapies, including active vitamin D or analogs with anti-oxidants and/or senolytics to ameliorate age-related conditions such as osteoporosis.

5. Conclusion

Active vitamin D insufficiency orchestrates a ROS $\rightarrow$ DNA damage $\rightarrow$ p16/SASP cascade that disrupts bone remodeling by suppressing osteoblastogenesis and enhancing osteoclastogenesis, culminating in trabecular deterioration and reduced bone mineral density. Restoring redox homeostasis with N-acetylcysteine, repleting 1,25-dihydroxyvitamin D_3, or genetically disabling p16 each reversed oxidative damage, dampened senescence, and normalized formation–resorption balance, thereby rescuing bone mass and microarchitecture. These findings establish a causal vitamin D–redox–senescence axis in skeletal aging and provide a preclinical rationale for investigating redox modulation and senescence control as potential therapeutic avenues. From a clinical perspective, ensuring physiological vitamin D sufficiency remains the foundational and proven approach. Our work suggests that targeting the downstream redox-senescence axis could, in the future, offer a complementary strategy; however, we emphasize that this is a long-term prospect. The successful translation of such approaches would require robust clinical investigation and must first overcome significant known challenges, including target tissue-specific delivery, the determination of optimal dosage and duration, and rigorous assessment of long-term safety and off-target effects. Future studies should define cell type–specific mechanisms, integrate redox metabolomics with single-cell senescence mapping, and test combination interventions in primary and secondary osteoporosis models.

Availability of Data and Materials

The data that support the findings of this study are available from the corresponding author upon reasonable request.

Author Contributions

DM conceived and supervised the project, secured funding, provided research resources and facilities, validated findings, and led manuscript writing and revision. WQ performed primary experiments, analyzed data, and developed experimental methodologies. MH and LC conducted supporting experiments and assisted with data analysis and methodology development. DG made subbstantial contributions to the conception or design of the work and made critical revision to the article for important intellectual content. All authors approved the final version of this manuscript. All authors contributed to editorial changes in the manuscript. All authors have participated sufficiently in the work and agreed to be accountable for all aspects of the work.

Ethics Approval and Consent to Participate

The use of animals in this study was approved by the Institutional Animal Care and Use Committee of Nanjing Medical University (Approval number: IACUC-1802007), ensuring compliance with China's ethical guidelines for laboratory animal care and use.

Acknowledgment

Not applicable.

Funding

This work was supported by grants from the National Natural Science Foundation of China (81730066 to DM).

Conflict of Interest

The authors declare no conflict of interest.

References

[1] Hernlund E, Svedbom A, Ivergård M, Compston J, Cooper C, Stenmark J, *et al*. Osteoporosis in the European Union: medical management, epidemiology and economic burden. A report prepared in collaboration with the International Osteoporosis Foundation (IOF) and the European Federation of Pharmaceutical Industry Associations (EFPIA). Archives of Osteoporosis. 2013; 8: 136. https://doi.org/10.1007/s11657-013-0136-1.

[2] Compston JE, McClung MR, Leslie WD. Osteoporosis. Lancet (London, England). 2019; 393: 364–376. https://doi.org/10.1016/S0140-6736(18)32112-3.

[3] Childs BG, Durik M, Baker DJ, van Deursen JM. Cellular senescence in aging and age-related disease: from mechanisms to therapy. Nature Medicine. 2015; 21: 1424–1435. https://doi.org/10.1038/nm.4000.

[4] Farr JN, Xu M, Weivoda MM, Monroe DG, Fraser DG, Onken JL, *et al*. Targeting cellular senescence prevents age-related bone loss in mice. Nature Medicine. 2017; 23: 1072–1079. https://doi.org/10.1038/nm.4385.

[5] Kuilman T, Michaloglou C, Mooi WJ, Peeper DS. The essence of senescence. Genes & Development. 2010; 24: 2463–2479. https://doi.org/10.1101/gad.1971610.

[6] Wiley CD, Campisi J. From Ancient Pathways to Aging Cells-Connecting Metabolism and Cellular Senescence. Cell

Metabolism. 2016; 23: 1013–1021. https://doi.org/10.1016/j.cmet.2016.05.010.

[7] Bouillon R, Marcocci C, Carmeliet G, Bikle D, White JH, Dawson-Hughes B, *et al*. Skeletal and Extraskeletal Actions of Vitamin D: Current Evidence and Outstanding Questions. Endocrine Reviews. 2019; 40: 1109–1151. https://doi.org/10.1210/er.2018-00126.

[8] Carlberg C, Haq A. The concept of the personal vitamin D response index. The Journal of Steroid Biochemistry and Molecular Biology. 2018; 175: 12–17. https://doi.org/10.1016/j.jsbmb.2016.12.011.

[9] Haussler MR, Whitfield GK, Kaneko I, Haussler CA, Hsieh D, Hsieh JC, *et al*. Molecular mechanisms of vitamin D action. Calcified Tissue International. 2013; 92: 77–98. https://doi.org/10.1007/s00223-012-9619-0.

[10] Saramäki A, Diermeier S, Kellner R, Laitinen H, Vaïsänen S, Carlberg C. Cyclical chromatin looping and transcription factor association on the regulatory regions of the p21 (CDKN1A) gene in response to 1alpha,25-dihydroxyvitamin D3. The Journal of Biological Chemistry. 2009; 284: 8073–8082. https://doi.org/10.1074/jbc.M808090200.

[11] Gire V, Dulic V. Senescence from G2 arrest, revisited. Cell Cycle (Georgetown, Tex.). 2015; 14: 297–304. https://doi.org/10.1080/15384101.2014.1000134.

[12] Sharpless NE, Sherr CJ. Forging a signature of in vivo senescence. Nature Reviews. Cancer. 2015; 15: 397–408. https://doi.org/10.1038/nrc3960.

[13] Justice JN, Nambiar AM, Tchkonia T, LeBrasseur NK, Pascual R, Hashmi SK, *et al*. Senolytics in idiopathic pulmonary fibrosis: Results from a first-in-human, open-label, pilot study. EBioMedicine. 2019; 40: 554–563. https://doi.org/10.1016/j.ebiom.2018.12.052.

[14] Xu M, Pirtskhalava T, Farr JN, Weigand BM, Palmer AK, Weivoda MM, *et al*. Senolytics improve physical function and increase lifespan in old age. Nature Medicine. 2018; 24: 1246–1256. https://doi.org/10.1038/s41591-018-0092-9.

[15] Chen Y, Liu W, Sun T, Huang Y, Wang Y, Deb DK, *et al*. 1,25-Dihydroxyvitamin D promotes negative feedback regulation of TLR signaling via targeting microRNA-155-SOCS1 in macrophages. Journal of Immunology (Baltimore, Md.: 1950). 2013; 190: 3687–3695. https://doi.org/10.4049/jimmunol.1203273.

[16] Yang C, Chen L, Guo X, Sun H, Miao D. The Vitamin D-Sirt1/PGC1alpha Axis Regulates Bone Metabolism and Counteracts Osteoporosis. Journal of Orthopaedic Translation. 2025; 50: 211-222. https://doi.org/10.1016/j.jot.2024.10.011.

[17] Talati Z, Egnell M, Hercberg S, Julia C, Pettigrew S. Consumers' Perceptions of Five Front-of-Package Nutrition Labels: An Experimental Study Across 12 Countries. Nutrients. 2019; 11: 1934. https://doi.org/10.3390/nu11081934.

[18] Chen J, Zhang J, Li J, Qin R, Lu N, Goltzman D, *et al*. 1,25-Dihydroxyvitamin D Deficiency Accelerates Aging-related Osteoarthritis via Downregulation of Sirt1 in Mice. International Journal of Biological Sciences. 2023; 19: 610-624. https://doi.org/10.7150/ijbs.78785.

[19] Wimalawansa SJ. Vitamin D Deficiency: Effects on Oxidative Stress, Epigenetics, Gene Regulation, and Aging. Biology (Basel). 2019; 8: 30. https://doi.org/10.3390/biology8020030.

[20] Qiao W, Yu S, Sun H, Chen L, Wang R, Wu X, *et al*. 1,25-Dihydroxyvitamin D insufficiency accelerates age-related bone loss by increasing oxidative stress and cell senescence. American Journal of Translational Research. 2020; 12: 507–518.

[21] Sun H, Qiao W, Cui M, Yang C, Wang R, Goltzman D, *et al*. The Polycomb Protein Bmi1 Plays a Crucial Role in the Prevention of 1,25(OH)$_2$ D Deficiency-Induced Bone Loss. Journal of Bone and Mineral Research: the Official Journal of the American Society for Bone and Mineral Research. 2020; 35: 583–595. https://doi.org/10.1002/jbmr.3921.

[22] Yang C, Qiao W, Xue Q, Goltzman D, Miao D, Dong Z. The senolytic agent ABT263 ameliorates osteoporosis caused by active vitamin D insufficiency through selective clearance of senescent skeletal cells. J Orthop Translat. 2024; 49: 107-118. https://doi.org/10.1016/j.jot.2024.08.012.

[23] Yang C, Qiao W, Xue Q, Goltzman D, Miao D, Dong Z. The senolytic agent ABT263 ameliorates osteoporosis caused by active vitamin D insufficiency through selective clearance of senescent skeletal cells. Journal of Orthopaedic Translation. 2024; 49: 107–118. https://doi.org/10.1016/j.jot.2024.08.012.

[24] Miao D, Scutt A. Histochemical localization of alkaline phosphatase activity in decalcified bone and cartilage. The Journal of Histochemistry and Cytochemistry: Official Journal of the Histochemistry Society. 2002; 50: 333–340. https://doi.org/10.1177/002215540205000305.

[25] Herranz N, Gil J. Mechanisms and functions of cellular senescence. The Journal of Clinical Investigation. 2018; 128: 1238–1246. https://doi.org/10.1172/JCI95148.

[26] Baker DJ, Wijshake T, Tchkonia T, LeBrasseur NK, Childs BG, van de Sluis B, *et al*. Clearance of p16Ink4a-positive senescent cells delays ageing-associated disorders. Nature. 2011; 479: 232–236. https://doi.org/10.1038/nature10600.

[27] Kirkland JL, Tchkonia T. Senolytic drugs: from discovery to translation. Journal of Internal Medicine. 2020; 288: 518–536. https://doi.org/10.1111/joim.13141.

[28] Kobayashi EH, Suzuki T, Funayama R, Nagashima T, Hayashi M, Sekine H, *et al*. Nrf2 suppresses macrophage inflammatory response by blocking proinflammatory cytokine transcription. Nature Communications. 2016; 7: 11624. https://doi.org/10.1038/ncomms11624.

[29] Rached MT, Kode A, Silva BC, Jung DY, Gray S, Ong H, *et al*. FoxO1 expression in osteoblasts regulates glucose homeostasis through regulation of osteocalcin in mice. The Journal of Clinical Investigation. 2010; 120: 357–368. https://doi.org/10.1172/JCI39901.

[30] Sun YX, Xu AH, Yang Y, Li J. Role of Nrf2 in bone metabolism. Journal of Biomedical Science. 2015; 22: 101. https://doi.org/10.1186/s12929-015-0212-5.

[31] Liu L, Cheung TH, Charville GW, Rando TA. Isolation of skeletal muscle stem cells by fluorescence-activated cell sorting. Nature Protocols. 2015; 10: 1612–1624. https://doi.org/10.1038/nprot.2015.110.

[32] Zhang W, Qu J, Liu GH, Belmonte JCI. The ageing epigenome and its rejuvenation. Nature Reviews. Molecular Cell Biology. 2020; 21: 137–150. https://doi.org/10.1038/s41580-019-0204-5.

[33] Han J, Yang K, An J, Jiang N, Fu S, Tang X. The Role of NRF2 in Bone Metabolism - Friend or Foe? Frontiers in Endocrinology. 2022; 13: 813057. https://doi.org/10.3389/fendo.2022.813057.

[34] Atkins GJ, Findlay DM. Osteocyte regulation of bone mineral: a little give and take. Osteoporosis International: a Journal Established as Result of Cooperation between the European Foundation for Osteoporosis and the National Osteoporosis Foundation of the USA. 2012; 23: 2067–2079. https://doi.org/10.1007/s00198-012-1915-z.

[35] Yasuda H. RANKL, a necessary chance for clinical application to osteoporosis and cancer-related bone diseases. World Journal of Orthopedics. 2013; 4: 207–217. https://doi.org/10.5312/wjo.v4.i4.207.

[36] Lean JM, Davies JT, Fuller K, Jagger CJ, Kirstein B, Partington GA, *et al*. A crucial role for thiol antioxidants in estrogen-deficiency bone loss. The Journal of Clinical Investigation. 2003; 112: 915–923. https://doi.org/10.1172/JCI18859.

[37] Miao D, Goltzman D. Mechanisms of action of vitamin D in

delaying aging and preventing disease by inhibiting oxidative stress. Vitamins and Hormones. 2023; 121: 293–318.

[38] Bjelakovic G, Nikolova D, Gluud LL, Simonetti RG, Gluud C. Antioxidant supplements for prevention of mortality in healthy participants and patients with various diseases. The Cochrane Database of Systematic Reviews. 2012; 2012: CD007176. https://doi.org/10.1002/14651858.CD007176.pub2.

[39] Amador-Martínez I, Aparicio-Trejo OE, Aranda-Rivera AK, Bernabe-Yepes B, Medina-Campos ON, Tapia E, *et al*. Effect of N-Acetylcysteine in Mitochondrial Function, Redox Signaling, and Sirtuin 3 Levels in the Heart During Cardiorenal Syndrome Type 4 Development. Antioxidants (Basel, Switzerland). 2025; 14: 367. https://doi.org/10.3390/antiox14030367.

[40] Samuni Y, Goldstein S, Dean OM, Berk M. The chemistry and biological activities of N-acetylcysteine. Biochimica et Biophysica Acta. 2013; 1830: 4117–4129. https://doi.org/10.1016/j.bbagen.2013.04.016.

[41] Batman A, Altuntas Y. RISK OF HYPERCALCEMIA IN ELDERLY PATIENTS WITH HYPERVITAMINOSIS D AND INTOXICATION. Acta Endocrinologica (Bucharest, Romania: 2005). 2021; 17: 200–206. https://doi.org/10.4183/aeb.2021.200.

[42] Reddy JP, Li Y. Oncogene-induced senescence and its role in tumor suppression. Journal of Mammary Gland Biology and Neoplasia. 2011; 16: 247–256. https://doi.org/10.1007/s10911-011-9221-5.

[43] Coppé JP, Desprez PY, Krtolica A, Campisi J. The senescence-associated secretory phenotype: the dark side of tumor suppression. Annual Review of Pathology. 2010; 5: 99–118. https://doi.org/10.1146/annurev-pathol-121808-102144.

[44] Takayanagi H. Osteoimmunology: shared mechanisms and crosstalk between the immune and bone systems. Nature Reviews. Immunology. 2007; 7: 292–304. https://doi.org/10.1038/nri2062.

[45] Zhu R, Wan H, Yang H, Song M, Chai Y, Yu B. The Role of Senescence-Associated Secretory Phenotype in Bone Loss. Frontiers in Cell and Developmental Biology. https://doi.org/10.3389/fcell.2022.841612.

[46] Shen J, Wang Q, Mao Y, Gao W, Duan S. Targeting the p53 signaling pathway in cancers: Molecular mechanisms and clinical studies. MedComm. 2023; 4: e288. https://doi.org/10.1002/mco2.288.

[47] Muñoz-Espín D, Serrano M. Cellular senescence: from physiology to pathology. Nature Reviews. Molecular Cell Biology. 2014; 15: 482–496. https://doi.org/10.1038/nrm3823.

[48] Christakos S, Dhawan P, Verstuyf A, Verlinden L, Carmeliet G. Vitamin D: Metabolism, Molecular Mechanism of Action, and Pleiotropic Effects. Physiological Reviews. 2016; 96: 365–408. https://doi.org/10.1152/physrev.00014.2015.

[49] Holick MF. Vitamin D deficiency. The New England Journal of Medicine. 2007; 357: 266–281. https://doi.org/10.1056/NEJMra070553.

[50] Childs BG, Gluscevic M, Baker DJ, Laberge RM, Marquess D, Dananberg J, *et al*. Senescent cells: an emerging target for diseases of ageing. Nature Reviews. Drug Discovery. 2017; 16: 718–735. https://doi.org/10.1038/nrd.2017.116.

[51] Manolagas SC. From estrogen-centric to aging and oxidative stress: a revised perspective of the pathogenesis of osteoporosis. Endocrine Reviews. 2010; 31: 266–300. https://doi.org/10.1210/er.2009-0024.

[52] Hirota Y, Nakagawa K, Mimatsu S, Sawada N, Sakaki T, Kubodera N, *et al*. Nongenomic effects of 1alpha,25-dihydroxyvitamin D(3) on cartilage formation deduced from comparisons between Cyp27b1 and Vdr knockout mice. Biochemical and Biophysical Research Communications. 2017; 483: 359-365. https://doi.org/10.1016/j.bbrc.2016.12.139.

[53] Jones G. Pharmacokinetics of vitamin D toxicity. The American Journal of Clinical Nutrition. 2008; 88: 582S–586S. https://doi.org/10.1093/ajcn/88.2.582S.